

This is a preprint manuscript version of the published paper:

Divergent impact of endotoxin priming and endotoxin tolerance on macrophage responses to cancer cells. *Cellular Immunology* 411-412, 104934, 2025

ISSN 0008-8749,

<https://doi.org/10.1016/j.cellimm.2025.104934>.

(<https://www.sciencedirect.com/science/article/pii/S000887492500019X>)

¹Konkonika Roy, ¹Tomasz Jędrzejewski, ¹Justyna Sobocińska, ¹Paulina Spisz, ¹Bartosz Maciejewski, ²Nadine Hövelmeyer, ³Benedetta Passeri, ¹Sylwia Wrotek

Title: Divergent Impact of Endotoxin Priming and Endotoxin Tolerance on Macrophage Responses to Cancer Cells

¹ Department of Immunology, Faculty of Biology and Veterinary Sciences, Nicolaus Copernicus University, 1 Lwowska Street, Torun, 87-100, Poland

² Institute for Molecular Medicine, University Medical Center of the Johannes Gutenberg-University Mainz, Mainz, Germany

³ Pathology Unit, Department of Veterinary Science, University of Parma, Strada del Taglio 10, 43126 Parma, Italy

Abstract

Endotoxin tolerance (ET) is an adaptive phenomenon that arises from the sustained exposure of immune cells, such as macrophages, to endotoxins, such as lipopolysaccharide (LPS). Initially, when macrophages are activated by LPS, they produce inflammatory mediators that drive the primary immune response. However, this response is significantly diminished during the establishment of ET, creating an immunosuppressive environment. Such an environment can facilitate the development and progression of malignant conditions, including cancer.

Our research focused on the interactions between immune cells and the tumor microenvironment under ET conditions. Through comprehensive *in vivo* and *in vitro* studies

employing various research techniques, we have demonstrated that interactions between endotoxin-tolerant macrophages (Mo_{ET}) and cancer cells contribute to a pro-tumorigenic condition. Notably, we observed that Mo_{ET} adapt a pro-tumorigenic, immunosuppressive M2 phenotype (CD163 expression). These macrophages involves distinct metabolic pathways, not depending solely on glycolysis and oxidative phosphorylation. Furthermore, our *in vivo* findings revealed macrophage infiltration within tumors under both ET and non-ET conditions, highlighting the suppressed immune landscape in the presence of ET. These findings suggest that ET plays a pivotal role in shaping tumor-associated immune responses and that targeting ET pathways could offer a novel and promising therapeutic approach for cancer treatment.

Introduction

It is known that when primed with endotoxin, macrophages are more reactive and produce higher levels of inflammatory mediators upon subsequent stimulation, whereas endotoxin-tolerant macrophages have a blunted response and lower production of these mediators [1]. The effect of endotoxin-treated macrophages on cancer development has been explored [2,3], with interesting findings showing that endotoxin-tolerant macrophages create favourable conditions for tumour progression. It is much less known however, how such endotoxin-tolerant macrophages respond to contact with cancer cells.

One of the expected effects of endotoxin tolerance is a switch of macrophage polarization. Macrophage polarization refers to the process by which macrophages adapt to different functional states in response to various signals from their environment, including pathogen associated molecular patterns (PAMPs), such as bacterial endotoxin [2]. These states are broadly categorized into two main phenotypes: M1 (classically activated) [3,4] and M2 (alternatively activated) macrophages [5,6]. Each phenotype plays a distinct role in immune responses, inflammation and tissue homeostasis. Recognizing macrophage polarization is essential because it provides insight into the immune system's balance between pro-inflammatory and anti-inflammatory responses. This understanding is critical for developing targeted therapies for various conditions, including infections, chronic inflammatory diseases and cancer.

To identify macrophage polarization, various markers and factors indicative of different macrophage phenotypes can be assessed. These include cytokines, enzymes, surface markers and the production of reactive oxygen species (ROS). Each of these elements plays a role in distinguishing between different macrophage states. It is well known that interleukin (IL) 6,

tumour necrosis factor (TNF) α and IL-1 β are produced in high levels by M1 macrophages and are key indicators of the pro-inflammatory state [7]. They drive inflammation and help recruit other immune cells to sites of infection [8] or injury [9]. Enzymes such as inducible nitric oxide synthase (iNOS) [10,11] and cyclooxygenase-2 (COX-2) [12] are directly involved in the metabolic activities and responses of macrophages. For instance, iNOS catalyzes nitric oxide production, which plays a role in pathogen killing and inflammation [13], but can also contribute to tissue damage if overproduced, while COX-2 generates pro-inflammatory prostaglandins [14,15]. Reactive oxygen species, generated by various sources including NADPH oxidase, play a role in pathogen destruction and tissue damage, further amplifying the inflammatory response [16,17]. These enzymatic activities provide insights into the functional roles of macrophages in inflammation and tissue repair that surface markers alone cannot reveal. Finally, surface markers, such as CD80 and CD163 complement cytokine and enzymatic markers by providing additional specificity for identifying M1 and M2 macrophages. CD80 marks the pro-inflammatory M1 state [18], while CD163 is a hallmark of the anti-inflammatory M2 state [19,20].

This study aims to determine whether endotoxin tolerance triggers a shift in macrophage polarization and metabolism, focusing on evaluating the response of endotoxin-tolerant macrophages upon contact with cancer cells *in vitro*.

Materials and methods

Experimental animals

Female BALB/c mice of 6 – 8 weeks old were purchased from the Mossakowski Medical Research Centre of the Polish Academy of Sciences (Warsaw, Poland) and allowed to acclimatize for 14 days before experimentation. The animals were housed individually in polycarbonate cages within a controlled environment. The room was maintained at a consistent relative humidity of $50 \pm 10\%$ and a temperature of $24 \pm 1^\circ\text{C}$, with a 12-hour light-dark cycle, where lights were turned on at 7:00 a.m. Food and water were provided *ad libitum*. All procedures were approved by the Local Bioethical Committee for Animal Care in Bydgoszcz (Poland; permission no. LKE 50/2022)

Preparation of lipopolysaccharide (LPS) solution

Lipopolysaccharide (LPS) from *Escherichia coli* (strain O111:B4, Sigma-Aldrich) was dissolved in sterile phosphate-buffered saline (PBS) and was applied at a final concentration of 100 ng/mL for the experiments.

Induction of endotoxin tolerance and breast cancer in mice

Mice were injected with LPS 50 µg/kg i.p. for three consecutive doses to induce endotoxin tolerance, and on the day 4 along with the LPS injection the mice were inoculated with 2.5×10^4 4T1 cells s.c. on the right mammary gland. The mice were then monitored daily to document the tumour growth. After approximately 3 weeks the mice were sacrificed by overdosing them with Ketamine and the tumour tissues were obtained for further analysis.

Immunohistochemical analysis

The breast tumour tissues were obtained and fixed with 10% formalin for 24h. Samples were routinely processed, and 5-µm thick sections were stained using Mayer's hematoxylin and eosin (HE) and prepared for immunohistochemistry. The primary antibody MAC387 (sc-66204, monoclonal, host: mouse, Santa Cruz), was titrated according to the manufacturer's recommendations: 1:200 for MAC387. Briefly, after dewaxing–rehydration, tissue sections were exposed to antigen retrieval; then, sections were cooled at room temperature for 20 min before being soaked into 3% H₂O₂ for 12 min. Slides were rinsed twice in PBS, pH 7.4, followed by serum blocking with normal goat serum. Incubation with primary antibody was carried out overnight at 4 °C. After being washed twice in PBS, pH 7.4, the slides were incubated for 30 min with a biotinylated goat anti-rabbit, IgG antibody. Afterwards, a avidin–biotin complex (ABC) peroxidase kit (Vectastain, Elite, ABC-Kit PK-6100, Vector Labs, Burlingame, CA, USA) and 3'3'-diaminobenzidine (DAB) system (DAB-Kit-SK4100, Vector Labs) were used for the detection of antigen–antibody reactions. Nuclei were counterstained with Mayer's hematoxylin. For negative controls, the primary antibodies were replaced by rabbit or goat serum, or Balb/c ascitic fluid at corresponding concentrations. All the images were captured using Nikon Eclipse E800.

Cell culture

The murine macrophage cell line RAW 264.7 was sourced from the European Collection of Authenticated Cell Cultures (Salisbury, UK), while the breast cancer cell line 4T1 was obtained from the American Type Culture Collection (Manassas, VA, USA). All cell lines were cultured

in high-glucose Dulbecco's Modified Eagle's Medium (DMEM), supplemented with 10% fetal bovine serum (FBS), 100 µg/mL streptomycin, and 100 IU/mL penicillin (all from Merck, Darmstadt, Germany). Cell cultures were maintained at 37°C in a humidified atmosphere with 5% CO₂ and sub-cultured every 2 – 3 days. Adherent 4T1 cells were detached using 0.25% trypsin-EDTA solution (Merck) upon reaching 70 – 80% confluency, while RAW 264.7 cells were detached by gentle scraping.

Induction of endotoxin tolerance in RAW 264.7 macrophages

RAW 264.7 macrophages were seeded in a 24-well plate at a concentration of 2×10^5 cells/well in 2 mL of DMEM medium supplemented with 10% FBS and pre-incubated for 24 h. The cells were then maintained in the following three conditions: non-tolerant macrophages (M_{ONT}), tolerant macrophages (M_{OET}), or macrophages treated only once with LPS for 24h (M_{OLPS}), which were used as a positive control. To obtain M_{OET} cells, RAW 264.7 cells were stimulated for 24 h with 100 ng/mL of LPS, followed by a wash with PBS and further culturing in a similar dose of LPS-containing media for another 24 h. Finally, the media was removed and the cells were directly lysed with PureZOL™ RNA Isolation Reagent (Bio-Rad, Hercules, CA, USA). The samples were then collected and stored at -80°C for future gene expression analysis.

Analysis of cytokine expression by Quantitative Real-Time PCR

Total RNA was isolated from the samples by PureZOL™ RNA Isolation Reagent following the manufacturer's protocol and the reverse transcription was performed using 1 µg of total RNA and iScript™ cDNA Synthesis Kit following manufacturer's protocol. Real-Time PCR was performed in a final volume of 10 µL, with each reaction mixture consisting of cDNA, SsoAdvanced Universal SYBR Green Supermix and the PrimePCR™SYBR® Green Assay designed for IL-10 (Unique Assay ID: qMmuCED0044967), TNF-α (Unique Assay ID: qMmuCED0004141) and iNOS amplification. Amplification was carried out using the CFX Connect Real-Time PCR Detection System. For data normalization, the housekeeping gene GAPDH (Unique Assay ID: qMmuCED0027497) was used to ensure accuracy. The double delta Ct method ($2^{-\Delta\Delta Ct}$) was employed for data analysis. To check for non-specific primer binding, a melt curve analysis was performed during each qPCR run. All reagents used in the analysis of cytokine expression were purchased from Bio-Rad (Hercules, CA, USA).

Western blot analysis

To analyse the expression of COX-2 and CD14, RAW 264.7 cells were seeded at a density of 1×10^5 cells/well in 12-well plate and pre-incubated for 24h in 2mL of DMEM medium supplemented with 10% FBS. The three conditions of M_{ONT} , M_{OLPS} and M_{OET} were maintained as described previously. Finally, the cells were washed with ice-cold PBS and lysed using 100 μ L of a $1 \times$ RIPA buffer supplemented with 1% sodium dodecyl sulfate (SDS) and 0.5% protease inhibitor cocktail (all the reagents were procured from Merck). After mechanical homogenization, the lysates were centrifuged to remove cellular debris. The samples were then heated at 95°C for 5 min. Protein concentrations in the lysates were determined using the Pierce™ BCA Protein Assay Kit (Thermo Fisher Scientific, Waltham, MA, USA), following the manufacturer's protocol. Lysates were diluted with sample buffer to a final concentration of 30 μ g/mL, and 20 μ L of each sample was subjected to SDS-PAGE on 4 – 20% precast polyacrylamide gels (Bio-Rad). Proteins were transferred to nitrocellulose membranes and immunoblotted with specific primary antibodies, followed by secondary antibodies conjugated to horseradish peroxidase (HRP). Immunoreactive bands were detected using the SuperSignal West Pico substrate (Thermo Fisher Scientific), and densitometric analysis was performed using Image Lab Software 5.2.1 (Bio-Rad). The details about the antibodies used in this research are provided in the Table 1.

Table 1. List of the antibodies used for western blot analysis

Primary Antibodies				
Protein Name	Protein Symbol	Cat. No.	Source/ Isotope	Company
Cyclooxygenase 2	COX-2	#12282	Rabbit IgG	Cell Signaling Technology (Danvers, MA, USA)
CD14	CD14	#93882	Rabbit IgG	Cell Signaling Technology
Actin	Actb	612657	Mouse IgG	BD Bioscience (Franklin Lakes, NJ, USA)
Secondary Antibodies				
Target	Origin	Type of conjugate	Company	
Anti-Rabbit	Goat IgG	Peroxidase-conjugated Anti-Rabbit	Sigma Aldrich	
Anti-Mouse	Goat IgG	Peroxidase-conjugated Anti-Mouse	Jackson ImmunoResearch Laboratories, Inc. (West Grove, PA, USA)	

Preparation of conditioned media derived from 4T1 cancer cells

To prepare the conditioned media, 4T1 cells were seeded at a density of 1×10^6 cells in a 75 cm² cell culture flask and were maintained in DMEM high glucose supplemented with 10% FBS till 70 – 80 % confluency was reached. The cells were then washed with PBS and maintained in DMEM high glucose supplemented with 1% FBS for 24h. Finally, the supernatant was collected, centrifuged and filtered to remove any cell debris. The conditioned media was then aliquoted and stored at -80°C for further use.

Nitric oxide production analysis

The Griess reagent (modified) (Sigma-Aldrich) was used according to the manufacturer's protocol to evaluate nitric oxide production. The assay solution was prepared with ultrapure distilled water, with the analysis being conducted in the presence of standards ranging from 0.5 – 65 μM of NO_2^- . The Raw 264.7 cells were seeded at a density of 5×10^5 cells/well in 24-well plate and were maintained in the condition of M_{ONT} , M_{OLPS} and M_{OET} . After the development of endotoxin tolerance, the cells were treated with the conditioned media at concentrations of 10, 25 and 50% obtained from 4T1 cells ($\text{CM}_{4\text{T1}} (10-50\%)$) for 16h. After the treatment, the supernatants were collected, centrifuged to remove the cell debris and then mixed with an equal volume of Griess reagent. After 15 min, the absorbance was read using Synergy HT Multi-Mode microplate reader (BioTek Instruments, Winooski, VT, USA) at 540 nm.

Reactive oxygen species (ROS) production analysis

The level of ROS in M_{ONT} , M_{OLPS} and M_{OET} treated with $\text{CM}_{4\text{T1}} (50\%)$ was analysed using the H_2DCFDA (Sigma-Aldrich) staining, followed by flow cytometry analysis. The RAW 264.7 cells were seeded at a density of 5×10^5 cells/well in 6 well plate and pre-incubated for 24h in DMEM supplemented with 10% FBS. Then, the cells were stained with 20 μM H_2DCFDA followed by incubation for 30 min in the dark at 37°C. After that, the cells were washed with PBS twice, and stimulated for 24h with $\text{CM}_{4\text{T1}} (50\%)$. After the stimulation, the cells were harvested, washed thrice with PBS, and the fluorescence was detected by flow cytometry using BriCyte E6 (Mindray, Shenzhen, China) at an excitation wavelength of 488 nm and an emission wavelength of 525 nm. The data was presented as the ratio of the geometric mean of stimulated/control cells.

Surface markers analysis

To analyse the effect of cancer on the polarization of Mo_{ET}, the flow cytometry was performed using fluorescein isothiocyanate (FITC)-labelled anti-CD80 monoclonal antibody and allophycocyanin (APC)-conjugated anti-CD163 monoclonal antibody (Sony Biotechnology Inc., San Jose, CA, USA) staining. In this experiment, co-culture of 4T1 and RAW 264.7 cells (Mo_{NT}, Mo_{LPS} and Mo_{ET}) was performed using well inserts of 0.4 μm of pore size (SARSTEDT). The RAW 264.7 cells were seeded at the density of 2×10^5 cells/well in 24-well plate for 24h. The macrophages were then stimulated to obtain the Mo_{NT}, Mo_{LPS} and Mo_{ET}. After the stimulation, the media was removed, the cells were washed once with PBS and the co-culture inserts were placed gently in the wells. The 4T1 cells were then seeded at a concentration of 0.03×10^6 cells/insert. After 24h, the inserts were removed and the monolayer of the macrophages was washed with ice-cold PBS and then harvested by gentle scraping in 1 mL of PBS. After collecting the cells, three more washes with PBS and 10 min-lasting incubation with Mouse Seroblock FcR (Bio-Rad, Hercules, CA, USA) were performed. Following the incubation, staining with anti-CD80 and anti-CD163 antibodies was performed in the dark for 30 min. The cells were then washed again with PBS thrice to remove any unbound antibodies and were finally suspended in 500 μL of PBS. The analysis was performed using BriCyte E6 flow cytometer (Mindray, Shenzhen, China).

Cell viability analysis

To assess the viability of RAW 264.7 cells after exposure to various concentrations of CM_{4T1}, an MTT assay (3-(4,5-Dimethyl-2-thiazolyl)-2,5-diphenyl-2H-tetrazolium bromide; Sigma Aldrich) was conducted. The cells were plated in 96-well plates at a density of 3×10^3 cells per well and pre-incubated for 24 hours in DMEM supplemented with 10% FBS. Following the pre-incubation, the cells were treated with CM_{4T1} in 1% FBS/DMEM at concentrations of 10%, 25%, 50%, and 75% for 24 and 48 hours. After treatment, the cells were rinsed with PBS and incubated with a red phenol-free medium containing 0.5 mg/mL of MTT solution for 3 hours at 37°C. Once incubation was complete, the medium was removed, and 100 μL of DMSO was added to dissolve the formazan crystals. The plate was then placed on an orbital shaker for 15 minutes to ensure thorough mixing. Optical density was measured at 570 nm, with 630 nm as the reference wavelength, using a Synergy HT Multi-Mode Microplate Reader (BioTek Instruments, Winooski, VT, USA). The viability of the CM_{4T1}-treated cells was expressed as a percentage relative to cells incubated in complete DMEM medium containing varying concentrations (10%, 25%, 50%, or 75%) of conditioned media supplemented with 1% FBS.

Single Cell Energetic Metabolism by Profiling Translation Inhibition (SCENITH)

To analyse the metabolic profile of RAW 264.7 macrophages, the SCENITH was performed by seeding the macrophages at a density of 3×10^5 cells/well in 6-well plate for 24h. To obtain Mo_{ET} cells the macrophages were primarily stimulated with LPS for 24h and then challenged again for 2h. Mo_{LPS} cells were treated once with LPS for 2h. Then Mo_{NT}, Mo_{LPS} and Mo_{ET} cells were stimulated with CM_{4T1} (50%) for 4h. Finally, the cells were harvested and seeded in the 96-well plate at a density of 3×10^4 cells/well. Cells in each condition were then either treated with inhibitor of glycolysis, 2-Deoxy-D-glucose (2-DG) (100 mM) (Sigma-aldrige) or inhibitor of oxidative phosphorylation (OXPHOS) (Sigma-aldrige), Oligomycin (2 μ M) or both 2-DG and Oligomycin for 20 min at 37°C. After the metabolic inhibitors, cells were treated with puromycin (Sigma-aldrige) 10 μ g/mL for 30 min at 37°C. The cells were then washed in PBS supplemented with 2% FBS thrice and then incubated in Fc blockade (BioXcel) anti-mouse/CD16/CD32 solution for 15 min at 37°C followed by washing with PBS twice. Then, the surface staining with live cell staining dye (Invitrogen) was performed for 20–30 min at 4°C, followed by washing in PBS. After the surface staining, fixation and permeabilization of these cells was performed using FOXP3 Fixation and Permeabilization Buffer (Thermofisher eBioscience kit) according to the manufacturer's protocol. Finally, the intracellular staining with anti-puromycin antibody (MERCK) was performed for 1h. Cells were then washed with permeabilization buffer twice, resuspended in PBS and stored at 4°C till the analysis.

Results

Macrophages infiltration in tumour tissue is prominent in Endotoxin tolerant mice

Since it is unknown whether endotoxin-tolerant macrophages are able to infiltrate the tumor, we conducted this analysis in the mice with and without endotoxin tolerance.

Morphologically, the tumours, arised in treated mice, were consistent with tubular carcinoma high grade. The tubular differentiation was minimal, with occasional small lumina. Individual neoplastic cells have oval vesicular nuclei and a fairly extensive amount of cytoplasm. The anisocytosis and anisokaryosis were consistent. Within the interstitium the fibroblasts proliferation made a fine support stroma, with some vacuolated macrophages associated and very few scattered neutrophils and small lymphocytes. Aberrant mitosis were occasionally found.

The immunohistochemical analysis of the tumour sections in both the groups of mice were observed to be infiltrated with few macrophages, located mostly in the fine stromal support (Fig 1).

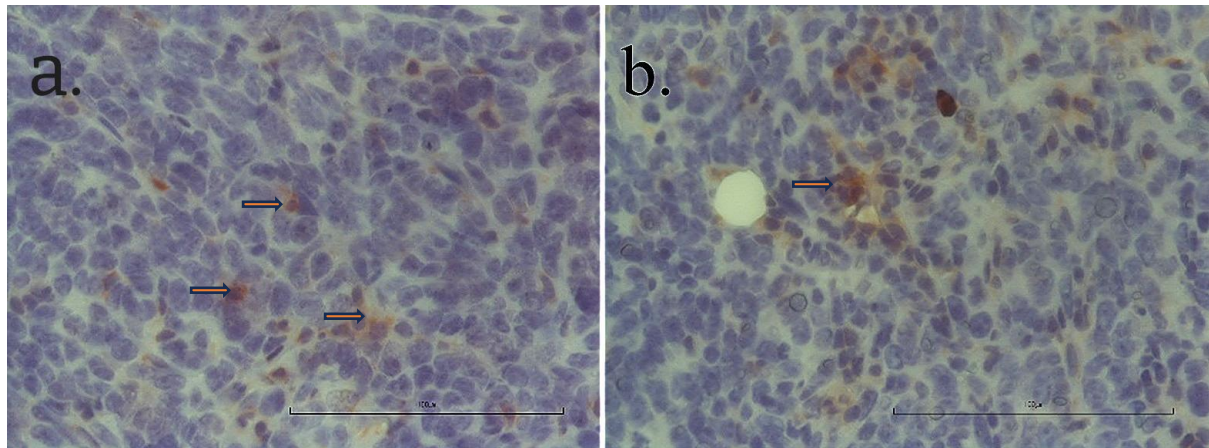


Fig 1. Immunochemical analysis of macrophage infiltration into breast cancer parenchyma (red arrow) and stroma (MAC387, 40X) in mice with cancer (a) and mice with ET and cancer (b). The analysis was performed in 6 individuals per group.

Considering that macrophages infiltrate tumors in both endotoxin-tolerant and non-tolerant mice, we continued our research on macrophages using an *in vitro* model of endotoxin tolerance.

Insight into the initiation and amplification of inflammation in response to single and prolonged endotoxin priming

In this research we exposed macrophages to endotoxin as we described in our previous paper [21] to get endotoxin-tolerant cells, which we verified by analysing IL-6 and TNF- α expression. After the initial exposure to endotoxin, we observed a significant increase ($p < 0.001$) in mRNA expression of both cytokines; however, this effect was evidently diminished with subsequent treatments of LPS (Fig. 2a-b). These changes observed are in parallel to the results of protein expression levels of TNF α and IL-6 observed also in our previous studies (Fig 2c-d).

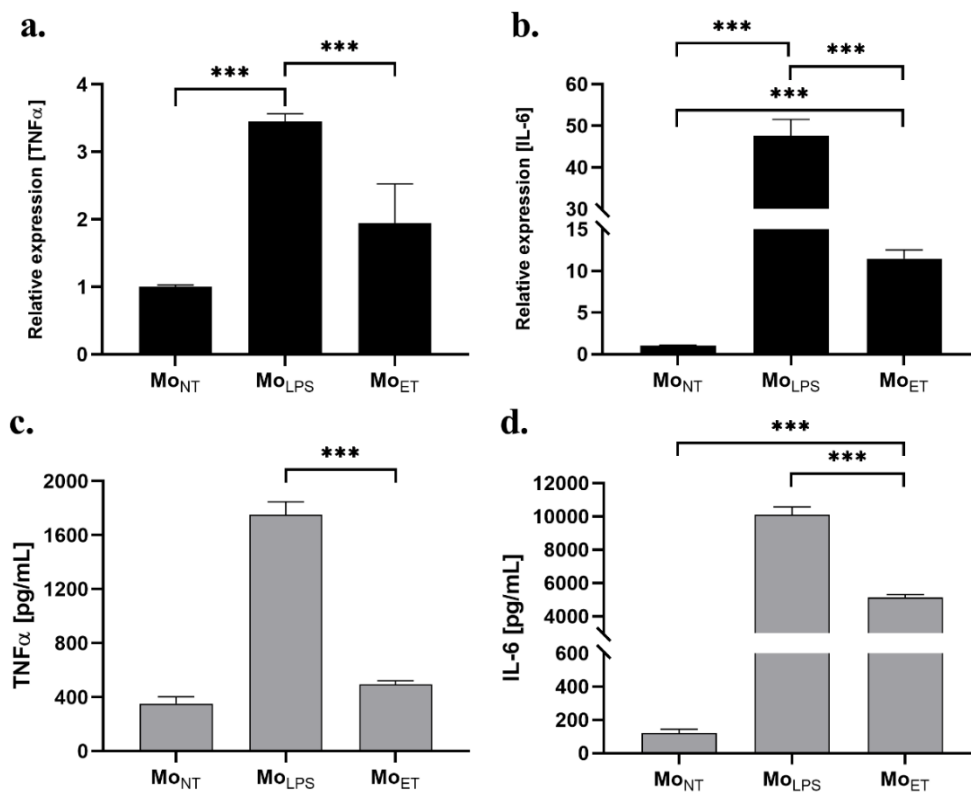


Fig. 2. The mRNA expression of TNF- α (a) and IL-6 (b) in response to RAW 264.7 macrophages priming with endotoxin and of the TNF- α (c) and IL-6 (d) levels in culture media from macrophages primed with endotoxin. Mo_{LPS} – macrophages treated with LPS once; Mo_{ET} – endotoxin tolerant macrophages; Mo_{NT} – untreated macrophages. Asterisks indicate significant differences between corresponding groups of cells as indicated (***) $p < 0.001$).

Having endotoxin tolerant (ET) cells, we decided to analyse CD14 and COX-2 to understand the underlying mechanisms. CD14 is crucial for the initial detection of endotoxins and the

subsequent activation of macrophages, leading to cytokine production. COX-2 is involved in the later stages of inflammation, where it synthesizes pro-inflammatory prostaglandins.

CD14 showed a downregulation trend in Mo_{ET} that was not found to be significant (Fig 3b). However, Mo_{ET} cells exhibited significantly lower production of COX-2 when compared to Mo_{LPS} ($p < 0.05$) (Fig. 3c).

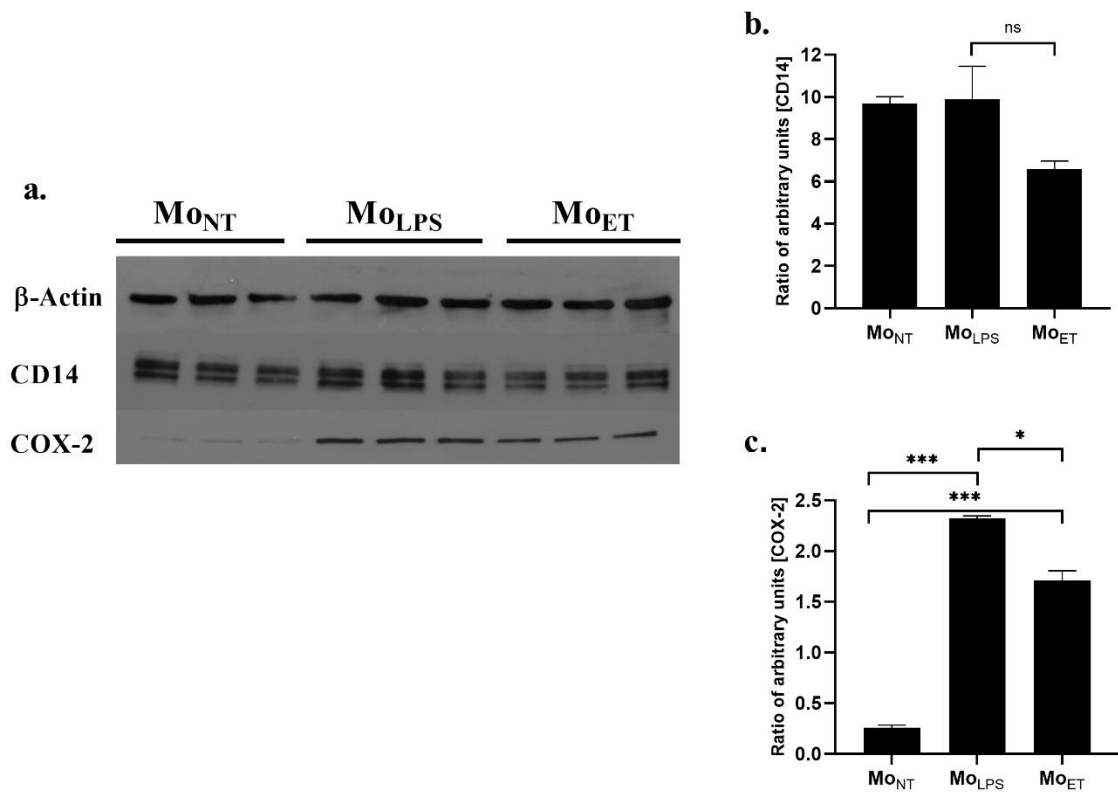


Fig.3. Expression of CD14 (b) and COX-2 (c) in endotoxin-treated RAW 264.7 macrophages. The levels of both proteins in the cell lysates were analysed by immunoblotting relative to β -actin content (a). Mo_{LPS} – macrophages treated with LPS once; Mo_{ET} – endotoxin tolerant macrophages; Mo_{NT} – untreated macrophages. Asterisks indicate significant differences between corresponding groups of cells as indicated (* $p < 0.05$ and *** $p < 0.001$).

Our research demonstrated that exposure of macrophages to endotoxins significantly affects factors involved in inflammation, and notably, this effect evolves over time.

Cancerogenic environment leads to a reduction in nitric oxide production by endotoxin-tolerant cells

Since it is known that cancer can significantly affect inflammation, we decided to investigate the effects of endotoxin and endotoxin tolerance in the context of cancer.

To further analyse new factors related to inflammation, we evaluated the production of nitric oxide (NO), which has been known to be regulated by similar pro-inflammatory signalling pathways, such as COX-2 involving nuclear factor (NF) κ B[22,23]. In this experiment, we wanted to analyze nitric oxide production in response to endotoxin exposure and then check it within a pro-carcinogenic environment. We observed a significantly inhibition of iNOS activity in Mo_{ET} after prolonged stimulation with LPS when compared to Mo_{LPS} ($p < 0.001$) (Fig. 4a). Therefore, in the next phase of the research, we examined, the production of nitric oxide (NO) by Mo_{ET} cells when stimulated with conditioned medium derived from cancer cells at a concentration from 10 to 50% (Fig. 4b). We found that Mo_{ET} cells stimulated with CM_{4T1} produced significantly lower concentrations of NO compared to Mo_{LPS} at corresponding doses of CM ($p < 0.001$) (Fig 4b).

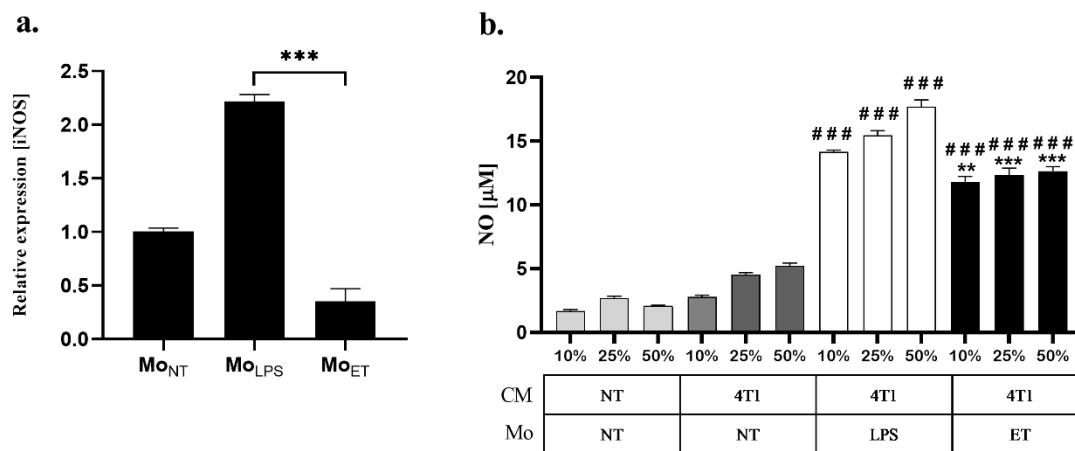


Fig. 4. The mRNA expression of iNOS in endotoxin-treated RAW 264.7 macrophages (a). Level of NO produced by endotoxin-treated macrophages stimulated with conditioned medium derived from 4T1 cancer cells (b). Mo_{LPS} – macrophages treated with LPS once; Mo_{ET} – endotoxin tolerant macrophages; Mo_{NT} – untreated macrophages; CM_{4T1} (10 - 50%) – conditioned media from 4T1 breast cancer cells. Asterisk (*) represents the significance against the Mo_{LPS} treated with CM_{4T1} (10 - 50%) (** $p < 0.01$ and *** $p < 0.001$) and hash (#) represents the significance against the Mo_{NT} treated with CM_{4T1} (10 - 50%) (### $p < 0.001$).

The cancerous environment enhances the capacity of endotoxin-tolerant cells to produce ROS in response to endotoxin, more so than in cells treated with LPS alone

As nitric oxide production and oxygen species (ROS) are involved in the the primary inflammatory response, we decided to investigate ROS production in the Mo_{ET} when they are in contact with a cancerous environment. In our study, we observed that conditioned medium from cancer cells does not affect Mo_{NT} ROS production. However, a higher level of ROS production was observed in Mo_{LPS} cells stimulated with CM_{4T1} at a concentration of 50% in comparison with Mo_{NT} ($p < 0.001$), and this increase was even more pronounced in Mo_{ET} cells ($p < 0.001$). The CM_{4T1} at 50% was used as a stimulant, as this represented a moderate concentration, neither excessively high nor too low (Fig. 5).

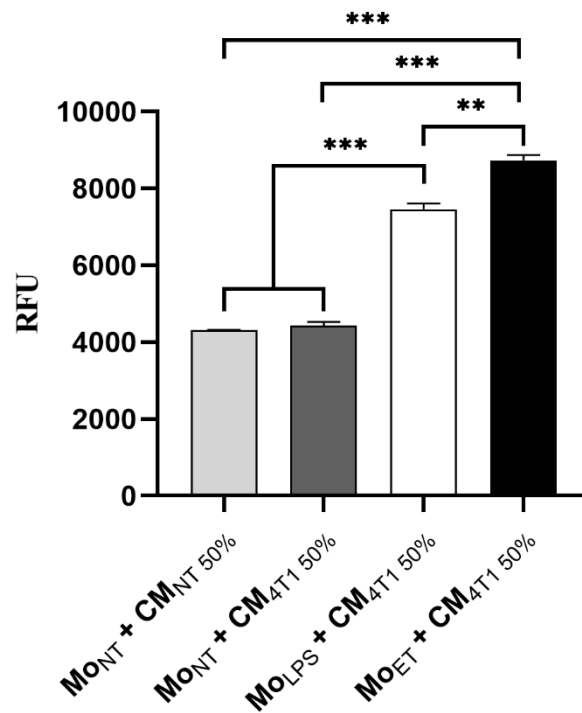


Fig 5. Intracellular level of ROS production in RAW 264.7 macrophages treated with LPS and cultured in conditioned medium from cancer cells. Flow cytometry analysis of ROS production is represented as MFI on Y axis of the graph. Mo_{LPS} – macrophages treated with LPS once; Mo_{ET} – endotoxin tolerant macrophages; Mo_{NT} – untreated macrophages; CM_{4T1} 50% - Conditioned media obtained from 4T1 cells. Asterisks indicate significant differences between corresponding groups of cells as indicated (***) $p < 0.001$).

Breast cancer influences the expression of surface markers on endotoxin-tolerant macrophages, shifting them towards an M2 phenotype

In our previous study, the Mo_{ET} cultured alone were observed to be majorly M1 phenotype due to the increased expression of CD80[21]. Since in this research we identified numerous functional changes in the macrophages exposed to endotoxin only once compared to those that develop endotoxin tolerance, we decided to assess their surface markers related to their phenotype. Here we evaluated the impact of breast cancer cells on these macrophages in a co-culture model. When co-cultured with 4T1 cells, Mo_{ET} cells showed significantly lower expression of CD80 compared to Mo_{NT} cells ($p < 0.05$) and Mo_{LPS} cells ($p < 0.01$) (Fig.6), and almost similar to the expression of CD80 in monoculture of Mo_{NT}. Interestingly, a significant increase in the expression of CD163, almost 10-fold, was observed in the Mo_{ET} cells during co-culture with 4T1 cancer cells in comparison with Mo_{NT} ($p < 0.001$) and Mo_{LPS} ($p < 0.01$) (Fig 6).

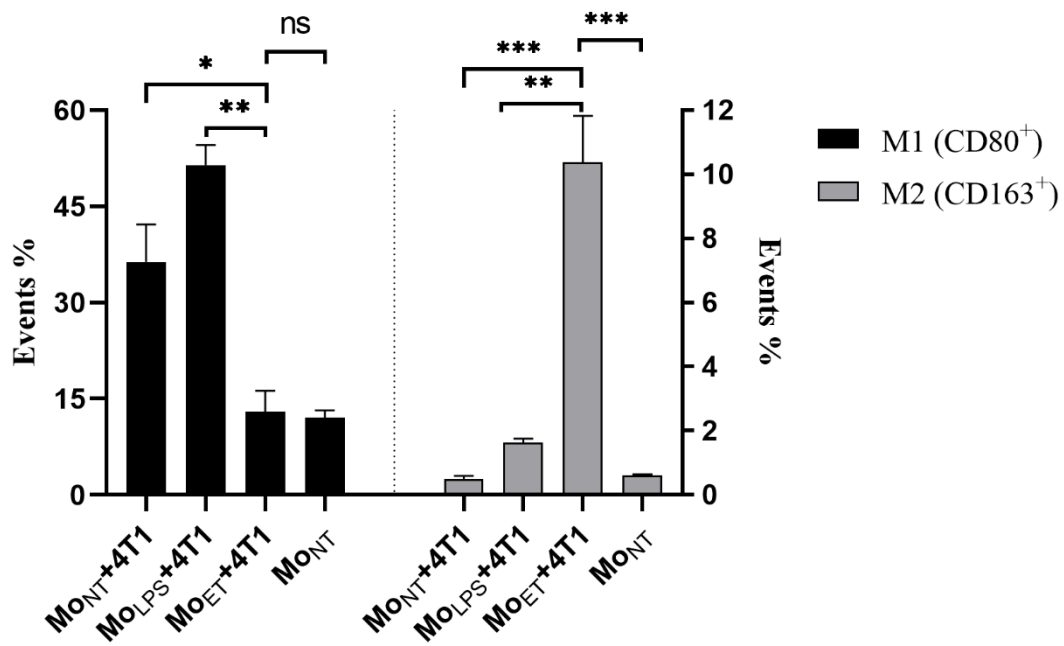


Fig 6. Evaluation of the phenotype of the RAW 264.7 macrophages (M1 and M2 markers) when co-cultured with 4T1 breast cancer cells. The % events of the M1 cells are plotted on the left Y-axis and the M2 cells are plotted on the right Y-axis. Mo_{LPS} – macrophages treated with LPS once; Mo_{ET} – endotoxin tolerant macrophages; Mo_{NT} – untreated macrophages. Asterisk (*) represents the significant differences in the corresponding groups as indicated (* $p < 0.05$, ** $p < 0.01$ and *** $p < 0.001$).

Endotoxin-tolerant macrophages demonstrate a greater increase in survival capacity in the presence of 4T1 cells compared to macrophages treated with LPS only once

To further assess the effect of cancer on endotoxin-tolerant macrophages, we studied the effect of the conditioned media derived from 4T1 cancer cells (at a concentration of 10, 25, 50 and 75%) on the following types of macrophages: M_{ONT} , M_{OLPS} and M_{OET} (Fig 7). M_{OET} cells, when stimulated with the CM_{4T1} , exhibited statistically significant increased survival capacity when compared to M_{ONT} and M_{OLPS} at both 24 (Fig 7a) and 48h (Fig 7b). Though there was a dose dependent decrease in the cell viability at 48h the viability % still remained >50% in case of M_{OET} cells stimulated with CM_{4T1} (50%) and was significantly higher when compared to M_{ONT} ($p < 0.01$) and M_{OLPS} ($p < 0.001$).

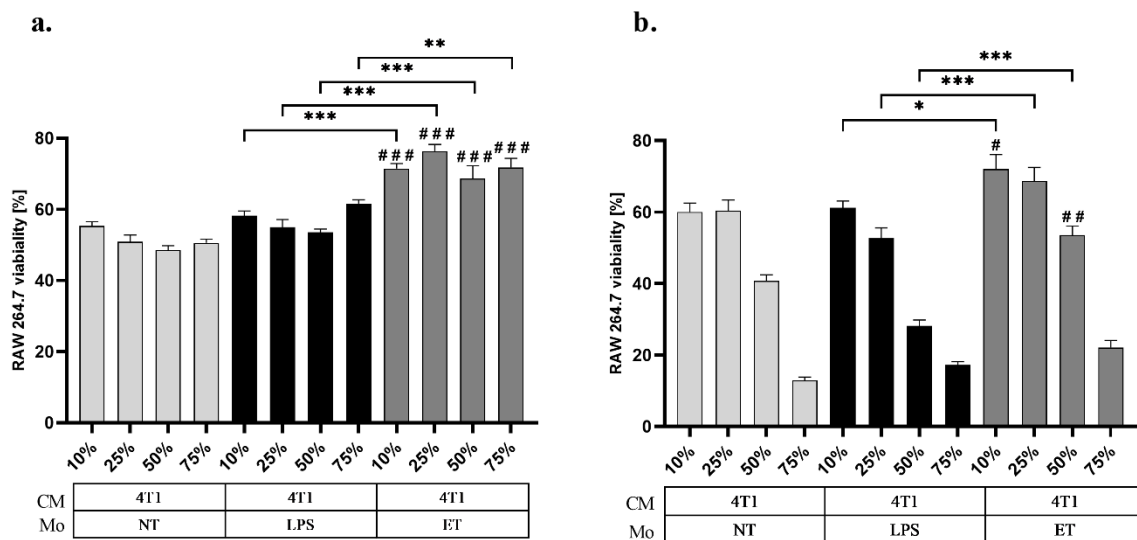


Fig 7. Viability of RAW 264.7 cells stimulated with conditioned media (CM) obtained from 4T1 at the concentration 10, 25, 50 and 75% for 24h (a) and 48h (b). Assessment of cell viability was done by colorimetric assay of MTT. The non-stimulated cells (which is represented as 100%) are used as the control to evaluate the percentage viability. Asterisk (*) represents the significance between M_{OET} and M_{OLPS} stimulated with the corresponding concentration of conditioned medium (10-75%) (* $p < 0.05$, ** $p < 0.01$ and *** $p < 0.001$). Hash (#) represents the significance of M_{OET} against the M_{ONT} stimulated with the corresponding concentration of conditioned medium (# $p < 0.05$, ## $p < 0.01$ and ### $p < 0.001$).

Endotoxin tolerance macrophages tend to have pronounced glycolytic activity

In this experiment, we decided to investigate the metabolic profile of these macrophages. SCENITH technique provides a way of measuring the dependence of cells on different metabolic pathways (glycolysis or oxidative phosphorylation). We observed a significant decrease in protein translation in RAW264.7 Mo_{NT} ($p < 0.001$) when treated with 2DG an inhibitor of glycolysis, when compared to the control cells not treated with the inhibitors (Baseline), indicating that these cells rely heavily on glycolysis for protein production (Fig. 8a). Conversely no significant decrease was observed in Mo_{LPS} and Mo_{ET}.

Interestingly, when treated with Oligomycin (an inhibitor of oxidative phosphorylation) Mo_{NT} ($p < 0.05$), Mo_{LPS} ($p < 0.05$) and Mo_{ET} ($p < 0.001$) exhibited a significant increase in the protein translation when compared to their respective baseline. This indicates that these ET macrophages do not strictly depend on OXPHOS and therefore, involvement of other metabolic pathway, such as the fatty acid oxidation or glutaminolysis has to be taken under consideration. Interestingly, Mo_{ET} treated with Oligomycin produced significantly higher protein when compared to Mo_{LPS} ($p < 0.001$). This finding suggests the activation of compensatory mechanisms that enhance protein production. Furthermore, this implies that endotoxin-tolerant macrophages respond differently to OXPHOS inhibition, possibly due to metabolic reprogramming associated with their tolerance state. Similarly, Mo_{NT}, Mo_{LPS} and Mo_{ET} when treated with CM_{4T1} produced similar results as on treatment with 2DG ($p < 0.001$) alone. However, when treated with oligomycin only Mo_{NT} ($p < 0.01$) and Mo_{ET} ($p < 0.001$) showed a prominent increase in the protein translation when compared to their respective baseline (Fig. 8b). We also observed that Mo_{LPS} and Mo_{ET} when stimulated with CM_{4T1} at a concentration of 50% also exhibited increased protein production when treated with Oligomycin than the Mo_{LPS} and Mo_{ET} alone ($p < 0.001$) (Fig 8c).

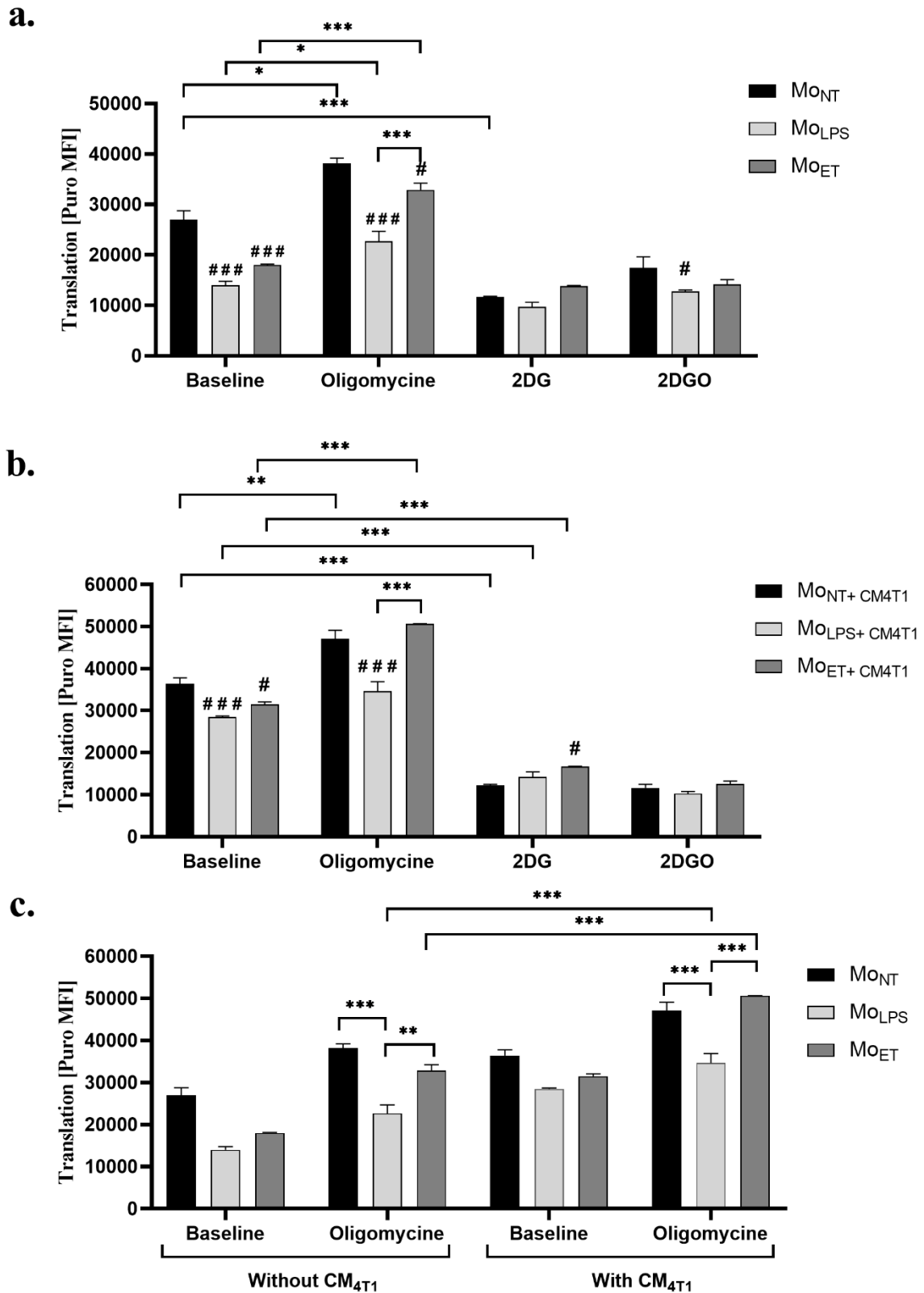


Fig 8. Evaluation of the metabolic activity of the RAW 264.7 macrophages (Mo_{NT}, Mo_{LPS} and Mo_{ET}) stimulated with conditioned media (CM) obtained from 4T1 at a concentration of 50%

by treating them with inhibitors Oligomycin, 2DG and puromycin. M_{ONT} – untreated macrophages; M_{OLPS} – macrophages treated with LPS once; M_{OET} – endotoxin tolerant macrophages. Flowcytometry was used to assess the protein translation MFI in M_{ONT} , M_{OLPS} and M_{OET} not stimulated with CM_{4T1} 50% (a), M_{ONT} , M_{OLPS} and M_{OET} stimulated with CM_{4T1} 50% (b) and Comparison of translation MFI on treatment with oligomycin between M_{ONT} , M_{OLPS} and M_{OET} stimulated with or without CM_{4T1} 50% (c). Asterisk (*) represents the significance of M_{OET} against the M_{OLPS} (* $p < 0.05$, ** $p < 0.01$ and *** $p < 0.001$) and hash (#) represents the significance of M_{OET} against the M_{ONT} (# $p < 0.05$, ## $p < 0.01$ and ### $p < 0.001$).

Overall, these findings illustrate the complex interplay between metabolic pathways and protein synthesis in different macrophage phenotypes. They highlight the reliance on glycolysis for protein production in M_{ONT} , M_{OLPS} and M_{OET} macrophages while suggesting that endotoxin tolerance allows for alternative metabolic adaptations. These metabolic shifts could provide tolerant macrophages with greater flexibility in adapting to LPS and different environmental challenges. Furthermore, the significant protein synthesis observed in response to oxidative phosphorylation inhibition underscores the potential for metabolic reprogramming in macrophages, particularly in the context of endotoxin tolerance, which may influence their functional roles in the tumour microenvironment.

Discussion

Endotoxin tolerance (ET) occurs when the immune system becomes less responsive to inflammatory signals induced by endotoxins following prolonged or repeated exposure[24,25]. Although commonly observed in conditions such as chronic infections, sepsis, or repeated medical treatments involving endotoxin exposure [26–28], ET remains a poorly studied phenomenon. Our previous study revealed that endotoxin-tolerant macrophages foster a cancer-friendly environment [21]. This study aims to further explore the impact of cancer cells on macrophages, specifically focusing on macrophage infiltration into tumors and functional changes in endotoxin-tolerant macrophages within the tumor microenvironment.

Macrophages are known to play a pivotal role within the tumor microenvironment and are also key cells in endotoxin tolerance [29,30]. While endotoxin tolerance is typically linked to immunosuppression and changes in macrophage function [31,32], its impact on macrophage infiltration into tumors remains unclear. Our findings show that tumor sections from tumor-bearing mice exhibited macrophage infiltration in both endotoxin-tolerant and non-tolerant groups, suggesting that ET does not prevent macrophage migration to the tumor site. However,

the functional state of these infiltrating macrophages under ET conditions remained uncertain. Therefore, we examined the behavior and characteristics of both endotoxin-tolerant (ET) and non-tolerant macrophages under controlled conditions, allowing for a detailed analysis of functional changes, including cytokine production, metabolic shifts, and surface marker expression, particularly in the context of cancer cell interactions.

Using an *in vitro* ET model, we delved into macrophage-cancer cell interactions. We observed that ET macrophages had reduced nitric oxide (NO) production and iNOS activity when exposed to cancer cell-conditioned medium, compared to normal and LPS-treated macrophages. This reduction in NO, which has a dual role in tumor biology promoting tumor growth at low levels and exerting cytotoxic effects at higher concentrations [33,34], suggests that ET macrophages create a tumor-favoring environment by limiting NO's cytotoxic potential [35]. In contrast, ET macrophages showed a significant increase in reactive oxygen species (ROS) production when stimulated with cancer cell-conditioned medium, pointing to an activation of oxidative stress pathways. This elevated ROS production aligns with tumor-promoting activities, as ROS can induce DNA damage and enhance cancer cell survival and metastasis [36–38].

These findings, *i.e.* increased ROS production (typically associated with pro-inflammatory M1 macrophages) alongside reduced NO levels (often linked to anti-inflammatory M2 macrophages) complicate the classification of ET macrophages as either M1 or M2. To further clarify, we examined surface markers, finding a shift in ET macrophages co-cultured with cancer cells, characterized by decreased CD80 expression and increased CD163 expression, suggesting an M2-like phenotype. This supports the view that tumor-associated macrophages (TAMs) often polarize toward an M2 phenotype, promoting immune suppression and tumor progression [39–41]. Additionally, ET macrophages displayed a blunted inflammatory response, with lower expression of pro-inflammatory cytokines like TNF- α and IL-6, reinforcing the notion that endotoxin tolerance shifts macrophages away from the M1 phenotype typically induced by single LPS exposure.

The paradox of increased ROS and decreased NO production in ET macrophages becomes more compelling when integrated with our SCENITH findings. Our SCENITH analysis revealed that ET macrophages are metabolically flexible, utilizing not only glycolysis but also pathways like fatty acid oxidation and glutaminolysis, especially when oxidative phosphorylation (OXPHOS) was inhibited. This metabolic adaptability may account for the

elevated ROS production, possibly as a byproduct of heightened metabolic activity in response to tumor signals, while downregulating NO production due to reprogramming of metabolic pathways.

Together, these findings indicate that the metabolic and functional adaptations in ET macrophages—highlighted through SCENITH and the analysis of ROS and NO production—equip them to support tumor growth dynamically, deviating from typical macrophage polarization patterns. This interplay between metabolic flexibility, ROS production, and NO regulation underscores the need to consider both metabolic and functional changes when studying macrophage behavior within the tumor microenvironment.

To further investigate ET macrophages' role in the tumor microenvironment, we examined their survival in tumor-associated stress conditions. We found that ET macrophages, often linked to an immunosuppressive phenotype (e.g., M2 polarization), displayed enhanced survival in cancer cell-conditioned media, indicating resilience to metabolic and inflammatory stresses common in tumors, such as nutrient deprivation or hypoxia. This suggests that ET not only modifies macrophage function but also confers a survival advantage, potentially allowing these cells to persist and impact the tumor's immune landscape in ways that non-tolerant macrophages cannot. This insight into ET macrophage persistence could shed light on their roles in chronic inflammation and cancer progression.

In conclusion, our findings suggest that conditions leading to endotoxin tolerance (ET) result in, on one hand, a change in the phenotypic characteristics of macrophages, and on the other hand, a shift in how they respond to cancer cells. The capacity of ET macrophages for tumor infiltration, ROS production, NO modulation, and metabolic adaptability highlights a functional reprogramming that may enhance their pro-tumor activity. These adaptations emphasize the complex relationship between inflammation, metabolic pathways, and tumor biology, suggesting new potential targets for therapeutic intervention.

References

1. Murphey, E.D.; Fang, G.; Sherwood, E.R. Endotoxin pretreatment improves bacterial clearance and decreases mortality in mice challenged with staphylococcus aureus. *Shock* **2008**, *29*, 512–518, doi:10.1097/SHK.0b013e318150776f.
2. Lichtnekert, J.; Kawakami, T.; Parks, W.C.; Duffield, J.S. Changes in Macrophage Phenotype as the Immune Response Evolves. *Curr. Opin. Pharmacol.* **2013**, *13*, 555–564, doi:10.1016/j.coph.2013.05.013.

3. Klar, A.S.; Michalak-Mińska, K.; Biedermann, T.; Simmen-Meuli, C.; Reichmann, E.; Meuli, M. Characterization of M1 and M2 Polarization of Macrophages in Vascularized Human Dermo-Epidermal Skin Substitutes in Vivo. *Pediatr. Surg. Int.* **2018**, *34*, 129–135, doi:10.1007/s00383-017-4179-z.
4. Zhu, Y.; Zhang, L.; Lu, Q.; Gao, Y.; Cai, Y.; Sui, A.; Su, T.; Shen, X.; Xie, B. Identification of Different Macrophage Subpopulations with Distinct Activities in a Mouse Model of Oxygen-Induced Retinopathy. *Int. J. Mol. Med.* **2017**, *40*, 281–292, doi:10.3892/ijmm.2017.3022.
5. Röszer, T. Understanding the Mysterious M2 Macrophage through Activation Markers and Effector Mechanisms. *Mediators Inflamm.* **2015**, *2015*, 816460, doi:10.1155/2015/816460.
6. De Paoli, F.; Staels, B.; Chinetti-Gbaguidi, G. Macrophage Phenotypes and Their Modulation in Atherosclerosis. *Circ. J.* **2014**, *78*, 1775–1781, doi:10.1253/circj.CJ-14-0621.
7. Novoselov, V.V.; Sazonova, M.A.; Ivanova, E.A.; Orekhov, A.N. Study of the Activated Macrophage Transcriptome. *Exp. Mol. Pathol.* **2015**, *99*, 575–580, doi:10.1016/j.yexmp.2015.09.014.
8. Davis, M.J.; Tsang, T.M.; Qiu, Y.; Dayrit, J.K.; Freij, J.B.; Huffnagle, G.B.; Olszewski, M.A. Macrophage M1/M2 Polarization Dynamically Adapts to Changes in Cytokine Microenvironments in *Cryptococcus Neoformans* Infection. *mBio* **2013**, *4*, e00264-13, doi:10.1128/mBio.00264-13.
9. Weidenbusch, M.; Anders, H.-J. Tissue Microenvironments Define and Get Reinforced by Macrophage Phenotypes in Homeostasis or during Inflammation, Repair and Fibrosis. *J. Innate Immun.* **2012**, *4*, 463–477, doi:10.1159/000336717.
10. Lisi, L.; Ciotti, G.M.P.; Braun, D.; Kalinin, S.; Currò, D.; Dello Russo, C.; Coli, A.; Mangiola, A.; Anile, C.; Feinstein, D.L.; et al. Expression of iNOS, CD163 and ARG-1 Taken as M1 and M2 Markers of Microglial Polarization in Human Glioblastoma and the Surrounding Normal Parenchyma. *Neurosci. Lett.* **2017**, *645*, 106–112, doi:10.1016/j.neulet.2017.02.076.
11. Al-Shaghдали, K.; Durante, B.; Hayward, C.; Beal, J.; Foey, A. Macrophage Subsets Exhibit Distinct E. Coli-LPS Tolerisable Cytokines Associated with the Negative Regulators, IRAK-M and Tollip. *PLOS ONE* **2019**, *14*, e0214681, doi:10.1371/journal.pone.0214681.
12. Linton, M.F.; Fazio, S. Macrophages, Inflammation, and Atherosclerosis. *Int. J. Obes.* **2003**, *27*, S35–S40, doi:10.1038/sj.ijo.0802498.
13. Kashfi, K.; Kannikal, J.; Nath, N. Macrophage Reprogramming and Cancer Therapeutics: Role of iNOS-Derived NO. *Cells* **2021**, *10*, 3194, doi:10.3390/cells10113194.
14. Sarkar, D.; Saha, P.; Gamre, S.; Bhattacharjee, S.; Hariharan, C.; Ganguly, S.; Sen, R.; Mandal, G.; Chattopadhyay, S.; Majumdar, S.; et al. Anti-Inflammatory Effect of Allylpyrocatechol in LPS-Induced Macrophages Is Mediated by Suppression of iNOS and COX-2 via the NF-κB Pathway. *Int. Immunopharmacol.* **2008**, *8*, 1264–1271, doi:10.1016/j.intimp.2008.05.003.

15. Ferrer, M.D.; Busquets-Cortés, C.; Capó, X.; Tejada, S.; Tur, J.A.; Pons, A.; Sureda, A. Cyclooxygenase-2 Inhibitors as a Therapeutic Target in Inflammatory Diseases. *Curr. Med. Chem.* **2019**, *26*, 3225–3241, doi:10.2174/0929867325666180514112124.
16. Chatterjee, S. Oxidative Stress, Inflammation, and Disease. In *Oxidative Stress and Biomaterials*; Elsevier, 2016; pp. 35–58 ISBN 978-0-12-803269-5.
17. Taylor, J.P.; Tse, H.M. The Role of NADPH Oxidases in Infectious and Inflammatory Diseases. *Redox Biol.* **2021**, *48*, 102159, doi:10.1016/j.redox.2021.102159.
18. Saradna, A.; Do, D.C.; Kumar, S.; Fu, Q.-L.; Gao, P. Macrophage Polarization and Allergic Asthma. *Transl. Res.* **2018**, *191*, 1–14, doi:10.1016/j.trsl.2017.09.002.
19. Dewhurst, J.A.; Lea, S.; Hardaker, E.; Dungwa, J.V.; Ravi, A.K.; Singh, D. Characterisation of Lung Macrophage Subpopulations in COPD Patients and Controls. *Sci. Rep.* **2017**, *7*, 7143, doi:10.1038/s41598-017-07101-2.
20. Ross, E.A.; Devitt, A.; Johnson, J.R. Macrophages: The Good, the Bad, and the Gluttony. *Front. Immunol.* **2021**, *12*, 708186, doi:10.3389/fimmu.2021.708186.
21. Roy, K.; Kozłowski, H.M.; Jędrzejewski, T.; Sobocińska, J.; Maciejewski, B.; Działuk, A.; Wrotek, S. Endotoxin Tolerance Creates Favourable Conditions for Cancer Development. *Cancers* **2023**, *15*, 5113, doi:10.3390/cancers15205113.
22. Al-Harbi, N.O.; Imam, F.; Al-Harbi, M.M.; Ansari, M.A.; Zoheir, K.M.A.; Korashy, H.M.; Sayed-Ahmed, M.M.; Attia, S.M.; Shabanah, O.A.; Ahmad, S.F. Dexamethasone Attenuates LPS-Induced Acute Lung Injury through Inhibition of NF- κ B, COX-2, and Pro-Inflammatory Mediators. *Immunol. Invest.* **2016**, *45*, 349–369, doi:10.3109/08820139.2016.1157814.
23. Lee, S.; Kwak, C.; Lee, S.; Ha, S.; Park, J.; Chung, T.; Ha, K.; Suh, S.; Chang, Y.; Chang, H.W.; et al. Anti-Inflammatory Effect of Ascochlorin in LPS-Stimulated RAW 264.7 Macrophage Cells Is Accompanied With the Down-Regulation of iNOS, COX-2 and Proinflammatory Cytokines Through NF- κ B, ERK1/2, and P38 Signaling Pathway. *J. Cell. Biochem.* **2016**, *117*, 978–987, doi:10.1002/jcb.25383.
24. Collins, P.E.; Carmody, R.J. The Regulation of Endotoxin Tolerance and Its Impact on Macrophage Activation. *Crit. Rev. Immunol.* **2015**, *35*, 293–323, doi:10.1615/CritRevImmunol.2015015495.
25. Nomura, F.; Akashi, S.; Sakao, Y.; Sato, S.; Kawai, T.; Matsumoto, M.; Nakanishi, K.; Kimoto, M.; Miyake, K.; Takeda, K.; et al. Cutting Edge: Endotoxin Tolerance in Mouse Peritoneal Macrophages Correlates with Down-Regulation of Surface Toll-Like Receptor 4 Expression. *J. Immunol.* **2000**, *164*, 3476–3479, doi:10.4049/jimmunol.164.7.3476.
26. Pena, O.M.; Hancock, D.G.; Lyle, N.H.; Linder, A.; Russell, J.A.; Xia, J.; Fjell, C.D.; Boyd, J.H.; Hancock, R.E.W. An Endotoxin Tolerance Signature Predicts Sepsis and Organ Dysfunction at Initial Clinical Presentation. *EBioMedicine* **2014**, *1*, 64–71, doi:10.1016/j.ebiom.2014.10.003.
27. Muthukuru, M.; Jotwani, R.; Cutler, C.W. Oral Mucosal Endotoxin Tolerance Induction in Chronic Periodontitis. *Infect. Immun.* **2005**, *73*, 687–694, doi:10.1128/IAI.73.2.687-694.2005.
28. Keel, M.; Schrengenberger, N.; Steckholzer, U.; Ungethum, U.; Kenney, J.; Trentz, O.; Ertel, W. Endotoxin Tolerance after Severe Injury and Its Regulatory Mechanisms. *J. Trauma Acute Care Surg.* **1996**, *41*, 430.

29. Hao, N.-B.; Lü, M.-H.; Fan, Y.-H.; Cao, Y.-L.; Zhang, Z.-R.; Yang, S.-M. Macrophages in Tumor Microenvironments and the Progression of Tumors. *J. Immunol. Res.* **2012**, *2012*, 948098, doi:10.1155/2012/948098.
30. Szebeni, G.J.; Vizler, C.; Kitajka, K.; Puskas, L.G. Inflammation and Cancer: Extra- and Intracellular Determinants of Tumor-Associated Macrophages as Tumor Promoters. *Mediators Inflamm.* **2017**, *2017*, 9294018, doi:10.1155/2017/9294018.
31. Pena, O.M.; Pistolic, J.; Raj, D.; Fjell, C.D.; Hancock, R.E.W. Endotoxin Tolerance Represents a Distinctive State of Alternative Polarization (M2) in Human Mononuclear Cells. *J. Immunol.* **2011**, *186*, 7243–7254, doi:10.4049/jimmunol.1001952.
32. Morris, M.; Li, L. Molecular Mechanisms and Pathological Consequences of Endotoxin Tolerance and Priming. *Arch. Immunol. Ther. Exp. (Warsz.)* **2012**, *60*, 13–18, doi:10.1007/s00005-011-0155-9.
33. Mocellin, S.; Bronte, V.; Nitti, D. Nitric Oxide, a Double Edged Sword in Cancer Biology: Searching for Therapeutic Opportunities. *Med. Res. Rev.* **2007**, *27*, 317–352, doi:10.1002/med.20092.
34. Singh, S.; Gupta, A.K. Nitric Oxide: Role in Tumour Biology and iNOS/NO-Based Anticancer Therapies. *Cancer Chemother. Pharmacol.* **2011**, *67*, 1211–1224, doi:10.1007/s00280-011-1654-4.
35. Thomsen, L.L.; Miles, D.W. Role of Nitric Oxide in Tumour Progression: Lessons from Human Tumours. *Cancer Metastasis Rev.* **1998**, *17*, 107–118, doi:10.1023/A:1005912906436.
36. Chen, A.; Huang, H.; Fang, S.; Hang, Q. ROS: A “Booster” for Chronic Inflammation and Tumor Metastasis. *Biochim. Biophys. Acta BBA - Rev. Cancer* **2024**, *1879*, 189175, doi:10.1016/j.bbcan.2024.189175.
37. Reuter, S.; Gupta, S.C.; Chaturvedi, M.M.; Aggarwal, B.B. Oxidative Stress, Inflammation, and Cancer: How Are They Linked? *Free Radic. Biol. Med.* **2010**, *49*, 1603–1616, doi:10.1016/j.freeradbiomed.2010.09.006.
38. Nathan, C.; Cunningham-Bussel, A. Beyond Oxidative Stress: An Immunologist’s Guide to Reactive Oxygen Species. *Nat. Rev. Immunol.* **2013**, *13*, 349–361, doi:10.1038/nri3423.
39. Nasrollahzadeh, E.; Razi, S.; Keshavarz-Fathi, M.; Mazzone, M.; Rezaei, N. Pro-Tumorigenic Functions of Macrophages at the Primary, Invasive and Metastatic Tumor Site. *Cancer Immunol. Immunother.* **2020**, *69*, 1673–1697, doi:10.1007/s00262-020-02616-6.
40. Goswami, K.K.; Ghosh, T.; Ghosh, S.; Sarkar, M.; Bose, A.; Baral, R. Tumor Promoting Role of Anti-Tumor Macrophages in Tumor Microenvironment. *Cell. Immunol.* **2017**, *316*, 1–10, doi:10.1016/j.cellimm.2017.04.005.
41. Griess, B.; Mir, S.; Datta, K.; Teoh-Fitzgerald, M. Scavenging Reactive Oxygen Species Selectively Inhibits M2 Macrophage Polarization and Their Pro-Tumorigenic Function in Part, via Stat3 Suppression. *Free Radic. Biol. Med.* **2020**, *147*, 48–60, doi:10.1016/j.freeradbiomed.2019.12.018.